Size-Exclusive Nanosensor for Quantitative Analysis of Fullerene C-60

ARTICLE *in* ENVIRONMENTAL SCIENCE & TECHNOLOGY · JUNE 2011

Impact Factor: 5.33 · DOI: 10.1021/es1043084 · Source: PubMed

6 AUTHORS, INCLUDING:

Veronica Okello
Binghamton University
13 PUBLICATIONS **48** CITATIONS
SEE PROFILE

Omowunmi Sadik
Binghamton University
142 PUBLICATIONS **2,958** CITATIONS
SEE PROFILE

Sarah Burns
Roswell Park Cancer Institute
7 PUBLICATIONS **23** CITATIONS
SEE PROFILE

Environmental Science & Technology

ARTICLE

pubs.acs.org/est

Size-Exclusive Nanosensor for Quantitative Analysis of Fullerene C_{60}

Samuel N. Kikandi, Veronica A. Okello, Qiong Wang, and Omowunmi A. Sadik*

Center for Advanced Sensors & Environmental System (CASE), Department of Chemistry, State University of New York-Binghamton, P.O. Box 6000 Binghamton, New York 13902-6000, United States

Katrina E. Varner

US-EPA/NERL Environmental Sciences Division, P.O. Box 93478-3478 Las Vegas, Nevada 89193-3478, United States

Sarah A. Burns

Department of Chemistry, 359 Natural Sciences Complex, State University of New York-Buffalo, Buffalo, New York 14260-3000, United States

Supporting Information

ABSTRACT: This paper presents the first development of a mass-sensitive nanosensor for the isolation and quantitative analyses of engineered fullerene (C_{60}) nanoparticles, while excluding mixtures of structurally similar fullerenes. Amino-modified *beta*-cyclodextrin (β-CD-NH_2) was synthesized and confirmed by ^{1}HNMR as the host molecule to isolate the desired fullerene C_{60}. This was subsequently assembled onto the surfaces of gold-coated quartz crystal microbalance (QCM) electrodes using *N*-dicyclohexylcarbodiimide/*N*-hydroxysuccinimide (DCC/NHS) surface immobilization chemistry to create a selective molecular configuration described as (Au)-S-$(CH_2)_2$-CONH-*beta*-CD sensor. The mass change on the sensor configuration on the QCM was monitored for selective quantitative analysis of fullerene C_{60} from a C_{60}/C_{70} mixture and soil samples. About $\sim 10^{14}-10^{16}$ C_{60} particles/cm^2 were successfully quantified by QCM measurements. Continuous spike of 200 μL of 0.14 mg C_{60} /mL produced changes in frequency ($-\Delta$f) that varied exponentially with concentration. FESEM and time-of-flight secondary−ion mass spectrometry confirmed the validity of sensor surface chemistry before and after exposure to fullerene C_{60}. The utility of this sensor for spiked real-world soil samples has been demonstrated. Comparable sensitivity was obtained using both the soil and purified toluene samples. This work demonstrates that the sensor has potential application in complex environmental matrices.

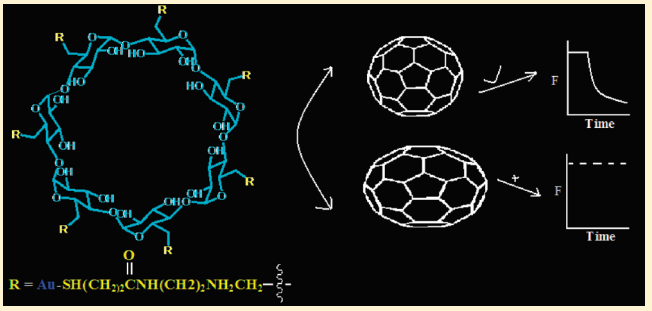

INTRODUCTION

The discovery of fullerenes in 1985 has ushered in an explosive growth in the applications of engineered nanomaterials (ENMs) and products.[1−5] The rapid development of nanotechnology and the increasing production of nanomaterials-based products and processes present great opportunities and challenges. To date, the potential impacts of nanomaterials on human health and the environment have been limited due to insufficient understanding of the risks associated with its development, manipulation and wide-ranging applications. The first step in assessing the risks posed by ENMs is to develop a broad array of analytical tools and methods that are applicable to a wide range of manufactured nanomaterials. Conventional methods of assessing the properties and characteristics of raw nanomaterials focus on the size distribution and effects. They are, however, unsuitable for detection and quantification of complex environmental samples or for differentiating between the total or dissolved metal fractions or metal oxidation states. The toxicity, detection and characterization of nanomaterials are dependent on factors such as functionalization, geometry, and the type of nanomaterials. For example, the cytotoxicity of fullerenes can be decreased following its hydroxylation with 24 hydroxyl groups,[3] while the cytotoxicity of carbon nanomaterials may be enhanced if it was functionalized with carboxylic acid moieties.[4] The potential toxicity of fullerenes and its derivatives is still a subject of intense discussion.[5] Some reports depict fullerenes as nontoxic while others demonstrate their ability to both quench and generate reactive oxygen species-(ROS),[6] which may lead to DNA damage.[7] Additionally,

Received: December 22, 2010
Accepted: May 10, 2011
Revised: May 4, 2011
Published: May 18, 2011

positive cytotoxicity and genotoxicity have been reported for the water-soluble C_{60} aggregates (nC_{60}) despite its low hydrophobicity.[8]

The first step to a better understanding of the fate and transport of fullerenes and other nanomaterials is to develop reliable metrology and analytical sensors. These offer novel screening and monitoring approaches toward a better understanding of engineered nanomaterials. Nanosensors can be classified under two main categories:[1,9] (i) Nanotechnology-enabled sensors or sensors that are themselves nanoscale or have nanoscale materials or components, and (ii) Nanoproperty-quantifiable sensors. Nanomaterials dimensions are on the same scale as biomolecules, which unveils exciting possibilities for their interaction with biological species, such as microbial, tissue, cells, antibodies, DNA, and other proteins. Type I sensors have been used for the construction of enzyme sensors, immunosensors, and genosensors, to achieve direct wiring of enzymes and relative components to electrode surface, to promote spectroelectrochemical reaction, to impose barcode for biomaterials and to amplify signal of biorecognition event[.[10,11] Extensive research papers and reviews using nanomaterials for chemical and bioassays have since been published.[1,5]

Despite the enormous literatures, there are few sensors to measure nanoscale properties or sensors belonging to Type II. This class of nanosensors is an area of critical interest to nanotoxicology, detection and risk assessment, as well as for monitoring of environmental and/or biological exposures to nanomaterials such as fullerene C_{60}. This is important because engineered fullerenes C_{60} which are prepared via thermal reactions always exist as a mixture of C_{60}, C_{70} and higher homologues. While supramolecular complexation with host−guest recognition is a well-studied topic,[12−14] and nanomaterials have been widely reported as components of sensing or other applications, to the best of our knowledge, there has neither been fullerene sensors reported nor the assembly of β-CD achieved onto mass selective transducers for C_{60} nanoparticle sensing applications. This paper presents the development of Category II nanosensor for the isolation and quantitative analyses of engineered fullerene C_{60} while excluding other structurally similar fullerenes C_{70} and higher homologues.

EXPERIMENTAL SECTION

Microgravimetric Measurements. Microgravimetric measurements were performed following a conventional procedure.[15] Briefly, all microgravimetric QCM experiments were performed using a QCA 917-quartz crystal analyzer (Seiko EG&G). This was an open circuit system where only the gold-coated quartz crystal (QA-A9M-Au(M)) from Advanced Measurement Technology (Oak Ridge, TN) working electrode (QCM, area ~0.2 cm^2) was connected in the absence of the auxiliary and the reference electrodes.). The resonators consisted of gold thickness layer of 300 nm and a frequency resolution of 0.1 Hz at a sampling rate of 100 ms, allowing excellent sensitivity down into the nanogram region. These resonators were mounted onto a Teflon well-type electrochemical cell[15] then soaked with test solutions. Buffalo River Sediments soil samples were obtained from, National Institute of Standards and Technology, Gaithersburg, MD 20899, (lot no. 8704).

Synthesis of Cyclodextrin Derivatives. The sensor fabrication started with the synthesis of β- or γ-cyclodextrin derivatives consisting of amino-functionalized derivatives of cyclodextrins designated as: β-CD-NH_2 **1** and γ-CD-NH_2 **2** (Supporting Information (SI) Figure 1A). The synthesis of these derivatives utilized previous literature procedures with slight modifications:[16] Briefly, 0.72 g of either β-CD or γ-CD was treated with 1.2 g toluene-2-sulfonyl chloride, TsCl (Sigma-Aldrich) and ethylenediamine(1 mL)(Sigma-Aldrich, US) in 20 mL pyridine (Sigma-Aldrich) and the mixture was refluxed for 7 h resulting in yellow solids. The yellow solids were designated as β-CD-NH_2, **1** or γ-CD-NH_2 **2**. These synthetic products (**1** and **2**) were stored under ultra high purity nitrogen (UHP) until they were utilized for the immobilization onto the QCM surface.

Successful synthesis of **1** and **2** were confirmed by ^{1}HNMR spectra recorded on a Bruker AM 360 spectroscopic system equipped with 8.45 T magnet and multinuclear and inverse detection capabilities at 360 MHz at 20 °C using D_2O solvent (SI Figure S1B). The ^{1}HNMR sample concentrations were approximated as 25 mg/mL of β-CD, β-CD-NH_2 **1**, γ-CD and γ-CD-NH_2 **2**. Compound **1**, showed characteristic NH_2 and methylene protons with chemical shifts at δ ~2.2 ppm and δ ~3.0 ppm respectively. Compound **2** showed similar chemical shifts at δ ~ 2.2 and 2.8 ppm for NH_2 and methylene protons respectively (data not included). Chemical shifts from both compounds **1** and **2** were consistent with the calculated theoretical chemical shifts values using ChemDraw for NH_2 and CH_2-protons (δ = 2.0 and δ = 2.8 ppm respectively). These results were consistent with literature precedence.[12,16,17] In addition, this modification is not only important for the immobilization chemistry but also for the enhanced cyclodextrin guest−host activity. For example, the depth of the cavity is extended from 0.78 to 1.10 nm and the hydrophilic nature of both ends of the β-CD cavity is changed due to the methyl groups attached to the O-2, O-3, or O-6 of the cyclodextrin.[18] Current work does not include studies on the effect of the cyclodextrin modification or did not eliminate the role of such chemistry in the sensor fabrication.

Cyclodextrin Assembly onto the QCM Transducer. Compounds **1** and **2** were immobilized separately on QCM via the DCC/NHS chemistry (Sigma-Aldrich).[15] First, QCM was cleaned in Piranha solution (H_2SO_4:H_2O_2 = 3:1, v/v) to remove any organic impurities and rinsed in copious amount of ethanol/water (1:1, v/v) mixture and dried gently in a stream of nitrogen. The cleaned QCM was subjected to the procedure shown in SI Figure S1C. Briefly, the QCM was soaked for 1 h in 1 mM 3, 3′ dithiopropionic acid, DTPA (Sigma-Aldrich) in acetone to facilitate the formation of the sensor molecular configuration hereby designated as QCM (Au)-S-$(CH_2)_2$-COOH acid **3**. The QCM with immobilized acid was rinsed again to remove any unreacted DTPA and then soaked in a mixture of 400 μL of 5 mM DCC (in acetone) plus 400 μL of ~5.0 mg/mL (in water) either β-CD-NH_2 **1** or γ-CD-NH_2 **2**. About 400 μL of 2 mM NHS (in acetone) was added and the conjugation reaction allowed for 30-60 min. During this conjugation process, carbodiimide molecule reacts with the carboxyl groups on the already immobilized DPTA molecule (via Au—S bond). This gives a highly reactive *O*-acylurea, which then reacts with the nucleophilic amines in **1** or **2** to form a stable amide.[19] NHS is added to stabilize the unstable carbodiimides.[19] The sensor was then rinsed to remove any excess reagents and dried gently in a stream of nitrogen. This modified QCM assembly was designated as QCM-S-$(CH_2)_2$-CONH-β-CD sensor, **4**.

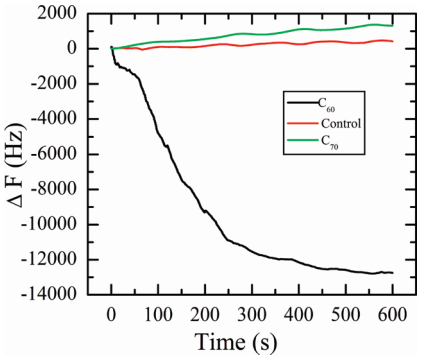

Figure 1. Change in frequency vs time for QCM (Au)-S-$(CH_2)_2$-CONH-*beta*-CD sensor, **4** in presence of fullerene 0.14 mg/mL C_{60}, C_{70} and control (toluene).

Isolation and Quantitation of Fullerene C_{60}. Several methods have been reported for separation of C_{60} especially in complex mixtures consisting of fullerene C_{70} and higher homologues.[5,20,21] Complexation of *beta*-cyclodextrin and fullerene C_{60} (β-CD-C_{60}) is known to be a tight fit compared to that of γ-CD-C_{60}.[18] The affinity is dictated by the CD cavity polarity and sizes as well as the stability constants. In aqueous solution the stability of the β-CD: C_{60} = 2: 1 complex is=1.696 × 10^5 dm^6 mol^{-2}), whereas that of γ-CD-C_{60} is k = 2.66 × 10^7 dm^6 mol^{-2}. This is a dynamic equilibrium that implies that C_{60} spends more time in β-CD cavity than that of γ-CD, an important consideration for the proposed nanosensor. The binding abilities and solubility for both C_{60} and C_{70} are higher in toluene solution.[22] Isolation and quantitation was achieved on a mass-sensitive QCM-S-$(CH_2)_2$-CONH-β-CD nanosensor, **4**. In solution, the complexation of C_{60}: β-CD = 1: 2 are favored (76%), 1: 1(61%) and 2:1(44%).[16] β-CD interaction with fullerenes is also selective because it complexes with C_{60}[19] and not with C_{70} or higher analogues.[16,23] This is because C_{60} (diameter ≈ 0.7 nm) is smaller than the internal diameter of β-CD cavity (diameter ≈ 0.79 nm) while that of C_{70} is larger (diameter ≈ 0.8 nm). While C_{60} is spherical, C_{70} is ovoid in shape which makes its recognition by β-CD more difficult (Scheme 1 SI). Therefore, when β-CD modified QCM sensor is exposed the mixture, C_{60} fits into the hydrophobic cavity while C_{70} is excluded on the basis of their size and shape. The sensor design was restricted to the isolation of C_{60} from this type of mixture because of its potential industrial practical utility and future improvement for environmental monitoring.

Nanosensor Measurements. The QCM (Au)A-S-$(CH_2)_2$-CONH-β-CD sensor, **4** was mounted to QCA 917-quartz crystal analyzer which was connected to EG&G PAR 263A potentiostat for data acquisition. In triplicates, exactly 200 μL of 0.14 mg/mL of C_{60} or C_{70} in toluene and control (toluene only) were placed on the modified QCM separately and the change in frequency was monitored over time. The changes were recorded as the immobilized β-CD on the QCM capturing the guest hydrophobic fullerene particles into their hydrophobic cavities.[12] These events[16] caused the resonant frequency to decrease in proportion to the mass according to Saurbrey equation $\Delta f = -((2fo^2))/s(\mu\rho)^{1/2})\Delta m$;[24]where Δf is the change in crystal frequency (which is the measured parameter), fo is the fundamental resonant frequency of the crystal (in the electrolyte), s is the electrode area (~ 0.2 cm^2), μ is the shear modulus of the crystal (=2.947 × 10^{11} g cm^{-1} s^{-2}), ρ is the density of the quartz (=2.648 g cm^{-3}) and Δm is the change in mass at the surface of the crystal resonator. Using this equation, frequency changes can be converted to adsorbed mass and finally converted to the number of captured C_{60} fullerene particles.[24]

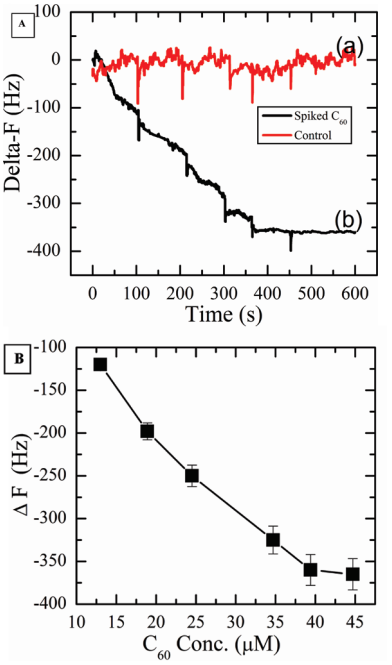

Figure 2. Dose-dependent response of QCM (Au)-S-$(CH_2)_2$-CONH-*beta*-CD sensor during the spiking of 200 μL of [A] (a) Control (toluene only) (b) 0.15 mg C_{60}/mL toluene: Arrows indicate the spiking events. [B] Change of frequency versus concentration of spiked C_{60} (μM).

Sensor Surface Characterization Using ToF−SIMS and FESEM. Time of flight−secondary ion mass spectrometry (ToF−SIMS) and field emission scanning electron microscope (FESEM), Zeiss Supra 55VP were used to characterize the surface chemistry during fabrication and testing experiments. Relevant details on the description of FESEM and ToF−SIMS are available in the SI: sensor surface characterization.

RESULTS AND DISCUSSION

Selective Fullerene C_{60} Quantitation using the Mass Sensor. As noted earlier, β-CD modified QCM sensor **4** was exposed to various concentrations of C_{60} or C_{70} in toluene. QCM relationship between the resonance oscillation frequency of piezoelectric crystal and interfacial mass change was monitored according to the Saurbrey equation.[24] A decrease in frequency of 1 Hz corresponds to 1.34 ng[25] and this was used to calculate the mass of the captured fullerenes. In this work, the sensor results are shown in Figure 1 when the sensor was exposed to 0.14 mg/mL of C_{60}, C_{70} and the control. Clearly, the sensor exposed to C_{60} showed significant decrease in frequency over time, whereas C_{70} and the control (toluene) remained relatively steady indicating that no significant mass was adsorbed on the QCM. This observation was consistent with the predicted sensor performance and it proved that it is indeed feasible and selective. The selective capture of C_{60} was not only feasible but was also found to be consistent with the expected β-CD-C_{60} guest−host interactions.[12,16] This is evident from the results. For example in Figure 1, the change in frequency was recorded as ~10618 Hz (or ~14228 ng), which corresponds to ~5.95 × 10^{16} C_{60} particles/cm^2. Using a 1:10 dilution, the observed Δf was

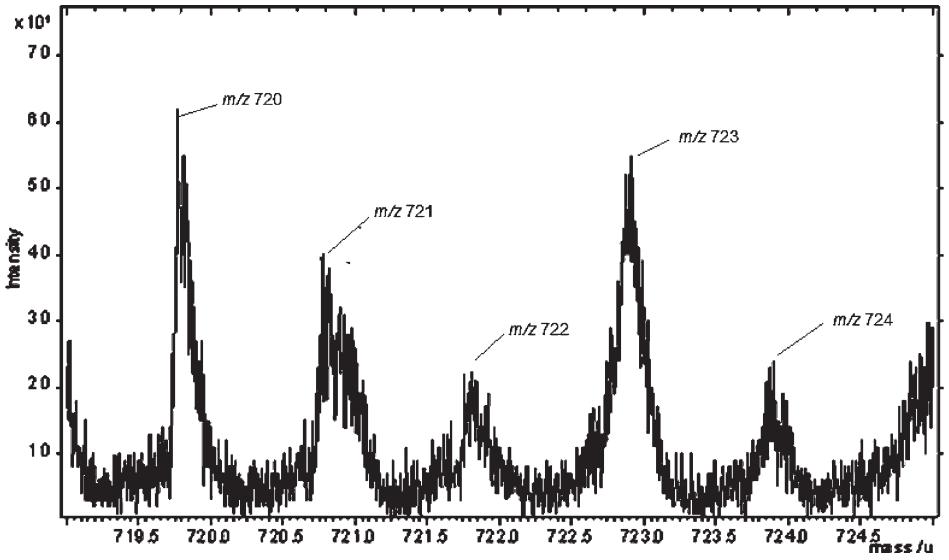

Figure 3. C_{60} mass at m/z 720 and isotopic peaks (m/z = 721, 722, 723, and 724). ToF−SIMS mass spectrum was acquired in the negative ion acquisition mode.

~1098.3 Hz (~ 1471.72 ng) or 6.15×10^{15} C_{60} particles/cm^2 and with a 1:100 dilution, the Δf was ~90.4 Hz, or 3.77×10^{14} C_{60} particles/cm^2. Overall, about $\sim 10^{14}-10^{16}$ C_{60} particles/cm^2 range was consistently quantified by this sensor from 0.14 mg C_{60} /mL solution at 1:1, 1:10 and 1:100 dilutions.

Assuming that a perfect β-CD (diameter = 0.78 nm) assembled on an active sensing electrode surface area of 0.2 cm^2, $\sim 1.90 \times 10^{14}$ β-CD/cm^2 should fit on the QCM sensor. If single C_{60} were isolated, $\sim 10^{14}$ C_{60}/cm^2 would be obtained from the observed results. However, the measured values were higher ($\sim 10^{14}-10^{16}$ C_{60}/cm^2) suggesting that both single nC_{60} and clusters, $(C_{60})_n$ had been captured since these exist as fractal system in toluene.[26] Also cyclodextrins are likely to coadsorb the fullerenes and solvent molecules or other trace impurities during the process. This coadsorption probably explains why the number frequency changes and measured particles were larger than anticipated. The discrepancy here was considered insignificant since the controls remained steady during measurements as evident from Figures 1 and 2. Similar variations were noted for DTPA during the sensor fabrication. The approximate number of DTPA and β-CD molecules calculated during the immobilization step was $\sim 3.3 \times 10^{15}$/ cm^2 and $\sim 5.9 \times 10^{14}$/ cm^2 respectively. The experimental number of β-CDs ($\sim 10^{14}$) and that of the predicted support molecules β-CD ($\sim 10^{14}$) were within the same order of magnitude. However, that of DTPA was 10-fold higher than β-CD, an indication that excess DTPA did not react with β-CD during the fabrication steps.

The quantitation of fullerene C_{60} nanoparticle was found to be consistent with other immobilized host−guest chemistry on similar QCM surface area. For example, Stobiecka and co-workers reported $\sim 10^{12}-10^{13}$ molecules/cm^2 of oligonucleotides immobilized on QCM.[25] It is obvious that the density of the immobilized molecules or particles on the electrode is expected to vary with their respective molecular sizes hence the slight variation observed. Additionally, this study also agrees with other works involving β-CD inclusion chemistries.[27]

Sensor Dose-dependent Response. Dose-dependent responses were subsequently tested using a conventional procedure.[15,28] A freshly fabricated QCM sensor modified with β-CD **4** was immersed into an electrochemical cell containing 6 mL of toluene and a stirring magnet. The cell was connected to quartz analyzer. The program and a timer were started simultaneously. Exactly, 200 μL of 0.15 mg C_{60}/mL or blank (toluene) were spiked separately at selected matching time intervals (100 s). Figure 2 shows the results obtained. Spiking of C_{60} solutions showed characteristic stair-case like profile along with decreasing frequency, whereas the control remained steady (Figure 2 (A)). The change in frequency ($-\Delta f$) varied exponentially with mass change (Δm) with R^2 = 0.998 (Figure 2(B)).

Fullerene C_{60} and C_{70} Interaction with γ-CD. In the previous section, it was demonstrated that β-CD (diameter = 0.78 nm) could selectively capture fullerene C_{60} (diameter = 0.7 nm) and not C_{70} (diameter = 0.8 nm) from toluene solution. Hypothetically, unlike β-CD, the use of γ-CD is expected to capture both C_{60} or C_{70} with no effect on the control. This is because of its larger cavity (diameter = 0.95 nm) compared to that of either the C_{60} or C_{70}. This hypothesis was tested by preparing the QCM sensor with γ-CD assembly in place of β-CD using the same procedure described earlier. The results obtained for C_{70} and C_{60} are shown in Figure S2(A) and (B)), respectively, under SI. As predicted, C_{60} and C_{70} were detected while the controls remained steady.

This is also consistent with the consideration that γ-CD cavity diameter is larger than the diameter C_{60} or C_{70}. γ-CD+C_{70} showed an ideal change in frequency where the decrease reaches a plateau as no more active binding sites (cavities) were available for C_{70}. It was predicted that a perfect γ-CD (diameter, d = 0.95 nm) has cavity surface area of about $\sim 7.1 \times 10^{-15}$ cm^2 each. Since the QCM area was approximated as 0.2 cm^2 then it is expected that up to $\sim 2.8 \times 10^{13}$ γ-CD particles/cm^2 would fit on the QCM sensor. Experimental results (Figure S2A in the SI) showed that in the presence of C_{70} a $\Delta F \sim -1836551$ Hz was obtained, which corresponds to $\sim 9.00 \times 10^{18}$ C_{70} particles/cm^2 captured. For C_{60}, ΔF was recorded as ~ -1242450 Hz, which corresponds to $\sim 7.1 \times 10^{18}$ C_{60} particles/cm^2. Obviously, these numbers of particles were higher than anticipated. This is consistent with earlier results of C_{60} detection by β-CD sensor,

an indication that both single and clustered or aggregated fullerenes were detected.[26] For a 1:20 concentration ratio of C_{60}/C_{70} mixture no interference was observed, however when the concentration of C_{70} was increased to 50 fold a lower number of C_{60} were captured on the sensor (Figure S2C in the SI)

Sensor Surface Characterization Using ToF-SIMS and FESEM. ToF-SIMS was used to determine if the fragmentation ions and spatial distribution of the attached molecules was actually achieved as predicted. This utilized low primary ion dosages (so-called static SIMS) to identify the molecular and fragment ions related to the gold substrate, DTPA, β-CD and the C_{60} components. The liquid metal ion source (Bi_n^{q+}) was used since this ion source can analyze a surface with high spatial resolution (to 50 nm) and with high sensitivity for molecular ion species.[29] The characteristic fragment ions identified in the static analysis were then used to construct the chemical images to identify the spatial distribution of these components. ToF-SIMS chemical imaging was initially used to determine if the chemical components of S-$(CH_2)_2$-CONH-β-CD were present at the surface of the gold substrate. This was achieved by analyzing the gold substrate before and after the functionalization chemistry. Once it was determined that the DTPA was present, a sample containing the acid component with the β-CD attached was analyzed to determine if both of these components were present and had similar spatial distribution. During this study it was observed that the acid and β-CD components formed surface domains in a similar spatial relation to the gold substrate and that these domains were also located in the same spatial arrangement as C_{60}.

This observation was followed by the identification of the characteristic fragment ions associated with the three major components of the sensor configuration: the gold substrate, the cyclodextrin, and fullerene (C_{60}). The gold ions formed a well characterized pattern in ToF-SIMS analysis which can be observed in a mass spectrum as clusters of gold (Au_n). The identified fragment ions associated with gold substrate were Au^-(m/z 197) and Au_3^-(m/z 591) while those associated with DTPA included $C_2H_4S^-$ (m/z 60); $C_3H_5SO_2^-$ (m/z 105); $C_6H_9S_2O_4^-$ (m/z 209) and $C_{12}H_{19}S_4O_8^-$ (m/z 419) as shown in SI Table S1 and Figure S3).The fragment loss of cyclodextrin has been described by Rabara and co-workers who utilized ToF-SIMS for the analysis of β-cyclodextrin and identified a series of fragment ions ($C_8H_{13}O_7^-$, $C_{14}H_{23}O_{12}^-$, $C_{20}H_{33}O_{17}^-$...) in the negative ion acquisition mode.[30] This fragmentation was observed in the formulated QCM and a mass spectrum of a representative cyclodextrin peak can be found in SI Table S2 and Figure S4.The fragment loss of C_{60} has previously been described as being a C_2 loss (C_{58}, C_{56}, C_{54}...) from the C_{60} initial mass.[31,32] This fragmentation loss pattern was not observed in the fullerene soaked QCM; only the peak for C_{60}^- at m/z 720 was observed (Figure 3). Other fragments associated with C_{60} included m/z 721, 722, 723, and 724 which is representative of the isotopic pattern of C_{60}. This was a critical step and the results confirmed that C_{60} had been captured from toluene by the sensor. In toluene, C_{60} is known to exist as a fractal system consisting of both single (C_{60}) and aggregates/clusters, $(C_{60})_n$.[26] Therefore, either single C_{60}, cluster $(C_{60})_n$ or both were isolated and measured by the sensor. While it is obvious for the detection of the single C_{60} particles by the predicted β-CD -C_{60} complexation, it is not so for the aggregated fullerenes, $(C_{60})_n$. In this work, ToF-SIMS results showed evidence of single fullerene particles (m/z 720) and the isotopic fragments. Detection of higher clusters of C_{60} proved to be difficult by ToF-SIMS due to the roughened surface which lowered the useable mass range of the sensors as observed. This however does not eliminate the possibility that C_{60} clusters exist at the surface.

FESEM (Zeiss SupraTM 55VP) was further used to provide evidence of such clusters on the sensor as long as they are at least within 1.7−4 nm range.[33] Fullerene clustering process is not clearly understood but available literature point to a radical mechanism since it is suppressed by addition of radical scavengers.[34] Formation of stable fullerene $(C_{60})_n$ clusters with sizes >1.2 nm in toluene solution and aggregation number $n \geq 3$ is known.[26] The number (n) is usually within $3 \leq n \geq 60$ with the spherical $(C_{60})_{55}$ cluster (4.6 nm) being the most stable.[26] Using the FESEM, the sensor was characterized and results showed presence of near spherical clusters ≥200 nm (SI Figure S5) suggesting a few hundreds of C_{60} particles per cluster. Overall, ToF-SIMS and FESEM confirmed the presence of both single and clustered C_{60} on the sensor consistent with the fractal system literature.[26]

Spatial Distribution. Chemical imaging of the ToF-SIMS data were used to determine the spatial distribution of the major components on the QCM during each phase of formulation. The images were analyzed using the Ion Image Software program and Image J, a public domain Java-based image processing program. The combination of these programs was used to study the fragments' spatial distributions.[35] The first sample analyzed contained the gold substrate treated with DTPA only. The chemical images indicated that the acid was present on the QCM surface with distinct segregation domains of DTPA fragment ions, which was attributed to roughened gold surfaces[36] (SI Figure S6A). The roughened surface could be a contributing factor in the characteristic uneven or patchy distribution of organic components during the QCM formulation process.[36−38] This suggested that subsequent imaging of the β-CD and C_{60} would most likely be located within these domains. In fact, SI Figure S6B shows some degree of shadowing in the overlaid image (c) since the intensity of Au in (a) appears a little blurred after attachment of the cyclodextrin.

The fully formulated QCM with the chemistry (Au)-S-$(CH_2)_2$-CONH-β-CD Sensor **4** was analyzed to determine if the intended reaction occurred with the cyclodextrin. The uneven distribution was again observed in the sample where there was segregation of the acid (DTPA) components to specific spatial domains on the gold substrate (SI Figure S6A(a)). Fragment ions associated with cyclodextrin were observed and distributed in the specific domains that were spatially correlated to the domain areas of the acid (DTPA) (SI Figure S6B(c)). The distribution of β-CD was more even over the surface versus either of the other components. The reason for this observation could be due to the reduced surface roughness that occurred once the DTPA had been conjugated to the Au surface of the QCM. The large molecular sizes of β-CD, along with the reduction in roughness would make them appear to be covering larger surface areas on the QCM without being restricted to the anchored acid sites. Atomic force microscopy (AFM) was used to determine if surface roughness was playing a role in the uneven distribution of the organic components as shown in SI Figure S7. The AFM images showed islands of materials spread out over the gold substrate in the same distribution indicated in the ToF−SIMS chemical images. The correlation between the ToF−SIMS and AFM data indicate that despite the uneven surface distribution, there was successful β-CD immobilization chemistry that was not observed in the controls.

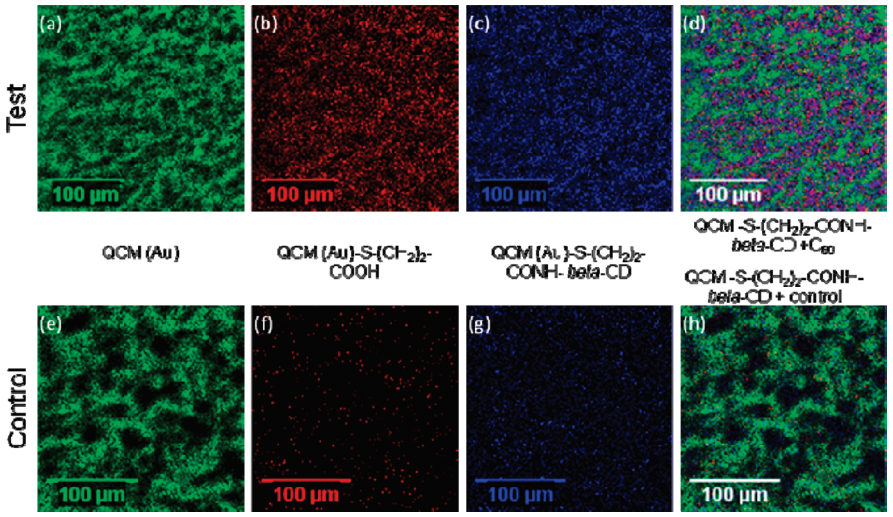

Figure 4. False color ToF−SIMS chemical image of QCM (Au)-S-$(CH_2)_2$-CONH-β-CD showing same stepwise sensor fabrication components (a−c and e−g) and overly of the three colored images after exposure to fullerene C_{60} (*d*) and control (*h*). Colored overlay image prepared using Ion Image Software Package, scale bar added using Image J.[35].

Finally, the sensor exposed to control and fullerene solutions were chemically imaged to determine the spatial distribution of the cyclodextrin and C_{60} fragment ions. Figure 4a−d or e−g represents initial sensor fabrication steps before exposure to C_{60} (Figure 6d) or control (Figure 4h). A keen examination of these figures show there was more shadowing of initial colors for Au, DTPA and β-CD after capturing C_{60} (Figure 4d) compared to the control (without C_{60}) (Figure 4h) from the colored overlay images. Additionally, the QCM exposed to the controls had very little signal from the C_{60} fragment ions in comparison with that exposed to fullerene solution. An insignificant ion signal was present in the control but was more likely due to baseline noise in the mass spectra as opposed to C_{60} fragment ions. The fullerene exposed QCM had a distribution of C_{60} fragment ions over the surface of the QCM that was consistent with the domain distribution of the cyclodextrin fragment ions. This confirms not only that the cyclodextrin and C_{60} are present on the surface of the QCM but also that they were spatially distributed in the same domains. Most importantly, this is the first report on successful immobilization of cyclodextrin on QCM surface for the purpose of quantifying engineered fullerene C_{60} particles

Environmental Application. Twelve mg of C_{60} and 10 mL of deionized water were added to 1 g of SRM soil samples and was stirred at 1150 rpm under ambient conditions for 1 h. One mL of anhydrous toluene was added and the resulting mixture was shaken for another 1 h. C_{60} was extracted into the organic phase. The extraction process was repeated 3 times with 1 mL of toluene. The resulting extract was filtered through a 0.20 μM filter membrane and diluted to make 0.14 mg/mL C_{60}. After capturing C_{60} particles onto the sensor from pure and soil samples, ΔF were 13251 and 9005 Hz, corresponding to 7.42×10^{16} and 5.04×10^{16} particles/cm^2, respectively (Figure 5). In both cases, similar orders of magnitude of the C_{60} particles/cm^2 were obtained.

Conclusion. We have demonstrated a new analytical concept that can be used to isolate and measure the number of engineered fullerene C_{60} particles from pure and soil samples. Mixtures containing C_{60}/C_{70} were isolated up to 20-fold C_{70} concentration. Utilizing QCM's mass detection capabilities, we have developed a Category II nanosensor concept based on supramolecular complexation of engineered fullerene nanoparticle onto cyclodextrin. The sensor provides a size-exclusive approach for quantitative analysis of the nominated fullerenes. To the best of our knowledge, this is the first Category II nanosensor reported for monitoring engineered fullerene C_{60}. The structural and morphological validity of the proposed sensor was confirmed using SIMS, NMR and SEM techniques, and the concept should be applicable to other fullerenes based on unique design of the sandwich configuration. We have thus discovered a new practical measurement method for engineered fullerenes C_{60}. Future work will focus on the application of the proposed sensor concept in wastewater samples, consumer products and food supplements.

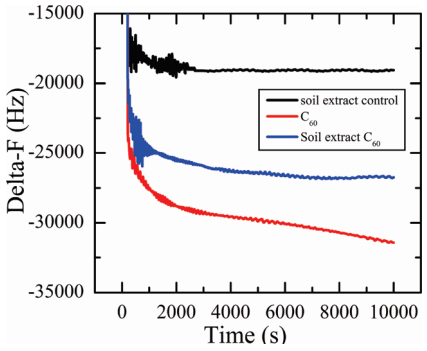

Figure 5. Change in frequency *vs* time for QCM (Au)-S-$(CH_2)_2$-CONH-*beta*-CD sensor, **4** in presence of fullerene 0.14 mg/mL C_{60}, C_{60} soil extract and control (toluene soil extract).

■ ASSOCIATED CONTENT

Supporting Information. Additional information on sensor synthesis, chemistry, characterization using ToF−SIMS and response to C_{70} and C_{70}/C_{60} mixture. (Figures S1−S7; Tables S1, S2; Scheme 1). This material is available free of charge via the Internet at http://pubs.acs.org.

AUTHOR INFORMATION

Corresponding Author
*Phone: (607)777-4132; fax:(607)777-4132, e-mail:osadik@binghamton.edu.

ACKNOWLEDGMENT

We acknowledge the U.S. Environmental Protection Agency for financial support through the STAR program (RD-83409101). SK also acknowledges the financial support of the Agency under the Student Services Contract No. RFQ-RT-08-00130.

REFERENCES

(1) Sadik, O. A.; S., K.; Wang, C. Q.; Varner, K. Sensors as tools for quantitation, nanotoxicity and nanomonitoring assessment of engineered nanomaterials. *J. Environ. Monit.* **2009**, *11*, 1782–1800.

(2) Nanotechnology White Paper. http://www.epa.gov/osa/pdfs/nanotech/epa-nanotechnology-whitepaper-0207.pdf (accessed May 17, 2011).

(3) Yamawaki, H.; Iwai, N. Cytotoxicity of water-soluble fullerene in vascular endothelial cells. *Am. J. Physiol.-Cell Physiol.* **2006**, *290* (6), C1495–C1502.

(4) Yang, X. L.; Fan, C. H.; Zhu, H. S. Photo-induced cytotoxicity of malonic acid [C60]fullerene derivatives and its mechanism. *Toxicol. In Vitro* **2002**, *16* (1), 41–46.

(5) Isaacson, C. W.; Kleber, M.; Field, J. A. Quantitative analysis of fullerene nanomaterials in environmental systems: A critical review. *Environ. Sci. Technol.* **2009**, *43* (17), 6463–6474.

(6) Sayes, C. M.; Fortner, J. D.; Guo, W.; Lyon, D.; Boyd, A. M.; Ausman, K. D.; Tao, Y. J.; Sitharaman, B.; Wilson, L. J.; Hughes, J. B.; West, J. L.; Colvin, V. L. The differential cytotoxicity of water-soluble fullerenes. *Nano Lett.* **2004**, *4* (10), 1881–1887.

(7) Isakovic, A.; Markovic, Z.; Todorovic-Markovic, B.; Nikolic, N.; Vranjes-Djuric, S.; Mirkovic, M.; Dramicanin, M.; Harhaji, L.; Raicevic, N.; Nikolic, Z.; Trajkovic, V. Distinct cytotoxic mechanisms of pristine versus hydroxylated fullerene. *Toxicol. Sci.* **2006**, *91* (1), 173–183.

(8) Zakharenko, L. P.; Zakharov, I. K.; Vasyunina, E. A.; Karamysheva, T. V.; Danilenko, A. M.; Nikiforov, A. A. Determination of genotoxicity of fullerene C-60 and fullerol by the somatic mutation and recombination test in *Drosophila melanogaster* and SOS chromotest. *Genetika* **1997**, *33* (3), 405–409.

(9) Sadik, O. A. Detecting engineered nanomaterials. *J. Environ. Monit.* **2007**, *9* (11), 1154–1154.

(10) Andreescu, S.; Njagi, J.; Ispas, C.; Ravalli, M. T. JEM Spotlight: Applications of advanced nanomaterials for environmental monitoring. *J. Environ. Monit.* **2009**, *11*, 27–40.

(11) Wei, D.; Bailey, M. J. A.; Andrew, P.; Ryhanen, T. Electrochemical biosensors at the nanoscale. *Lab Chip* **2009**, *9* (15), 2123–2131.

(12) Murthy, C. N.; Geckeler, K. E. The water-soluble beta-cyclodextrin-[60]fullerene complex. *Chem. Commun.* **2001**, *13*, 1194–1195.

(13) Giacalone, F.; D'Anna, F.; Giacalone, R.; Gruttadauria, M.; Riela, S.; Noto, R. Cyclodextrin-[60]fullerene conjugates: synthesis, characterization, and electrochemical behavior. *Tetrahedron Lett.* **2006**, *47* (46), 8105–8108.

(14) T. Anderson, K. N.; Sundahl, M.; Westman, G.; Wennerström, O. *J. Chem. Soc., Chem. Commun.* **1992**, 604–606.

(15) Aluoch, A. O.; Sadik, O. A.; Bedi, G. Development of an oral biosensor for salivary amylase using a monodispersed silver for signal amplification. *Anal. Biochem.* **2005**, *340*, 136–144.

(16) Liu, Y.; Yang, Y. W.; Chen, Y. Thio[2-(benzoylamino)-ethylamino-beta-CD fragment modified gold nanoparticles as recycling extractors for [60]fullerene. *Chem. Commun.* **2005**, *33*, 4208–4210.

(17) Nishijo, J.; Moriyama, S.; Shiota, S. Interactions of cholesterol with cyclodextrins in aqueous solution. *Chem. Pharm. Bull.* **2003**, *51* (11), 1253–1257.

(18) Murthy, C. N.; Geckeler, K. E. Stability studies on the water-soluble beta-cyclodextrin [60]fullerene inclusion complex. *Fullerenes, Nanotubes, Carbon Nanostruct.* **2002**, *10* (2), 91–98.

(19) Wrobel, N.; Schinkinger, M.; Mirsky, V. M. A novel ultraviolet assay for testing side reactions of carbodiimides. *Anal. Biochem.* **2002**, *305* (2), 135–138.

(20) Taylor, R., *Lecture Notes on Fullerene Chemistry: A Handbook for Chemists*; Imperial College Press: London, UK, 1999.

(21) Jinno, K., *Separation of Fullerenes by Liquid Chromatography*; The Royal Society of Chemistry: Cambridge, UK, 1999.

(22) Haino, T.; Yanase, M.; Fukunaga, C.; Fukazawa, Y. Fullerene encapsulation with calix[5]arenes. *Tetrahedron* **2006**, *62* (9), 2025–2035.

(23) Michal Lahav; Koodali T. Ranjit; Eugenii Katz; Willner, I., A b-amino-cyclodextrin monolayer-modified Au electrode: a command surfacefor the amperometric and microgravimetric transduction of optical signals recorded by a photoisomerizable bipyridinium−azobenzene diad. *Chem. Commun.* **1997**, *259*.

(24) Saurbrey, G. Z. *Z. Phys* **1959**, *155*, 206.

(25) Stobiecka, M.; Ciesla, J. M.; Janowska, B.; Tudek, B.; Radecka, H. Piezoelectric sensor for determination of genetically modified soybean roundup ready((R)) in samples not amplified by PCR. *Sensors* **2007**, *7* (8), 1462–1479.

(26) Bulavin, L. A.; Adamenko, I. I.; Yashchuk, V. M.; Ogul'chansky, T. Y.; Prylutskyy, Y. I.; Durov, S. S.; Scharff, P. Self-organization C60 nanoparticles in toluene solution. *J. Mol. Liq.* **2001**, *93* (1−3), 187–191.

(27) Lee, J. Y.; Park, S. M. Electrochemistry of guest molecules in thiolated cyclodextrin self-assembled monolayers: An implication for size-selective sensors. *J. Phys. Chem. B* **1998**, *102* (49), 9940–9945.

(28) Aluoch, A. O.; Amrute, K.; Sadik, O. A. Novel electrochemical oral biosensor for histatin. *Sensor Letters* **2005**, *3* (2), 161–163.

(29) Kollmer, F. Cluster primary ion bombardment of organic materials. *Appl. Surf. Sci.* **2004**, *231−232*, 153–158.

(30) Rabara, L.; Aranyosiova, M.; Velic, D. Supramolecular host-guest complexes based on cyclodextrin-diphenylhexatriene. *Appl. Surf. Sci.* **2006**, *525*, 7000–7002.

(31) O'Brien, S. C.; Heath, J. R.; Curl, R. F.; Smalley, R. E. Photophysics of buckminsterfullerene and other carbon cluster ions. *J. Chem. Phys.* **1988**, *88* (1), 220–232.

(32) Kato, N.; Yamashita, Y.; Iida, S.; Sanada, N.; Kudo, M. Analysis of ToF-SIMS spectra from fullerene compounds. *Appl. Surf. Sci.* **2008**, *225*, 938–940.

(33) http://www.zeiss.com/C1256E4600307C70/EmbedTitelIntern/SUPRA_VP_TechnicalData/$File/SUPRA_VP_Technical_Data.pdf. (accessed May 16, 2011).

(34) Rudalevige, T.; Francis, A. H.; Zand, R. Spectroscopic studies of fullerene aggregates. *J. Phys. Chem. A* **1998**, *102* (48), 9797–9802.

(35) Collins, T. J. ImageJ for microscopy. *BioTechniques* **2007**, *43*, S25–S30.

(36) Reimhult, K.; Yoshimatsu, K.; Risveden, K.; Chen, S.; Ye, L.; Rozer, A. Characterization of QCM sensor surfaces coated with molecularly imprinted nanoparticles. *Biosens. Bioelectron.* **2008**, *23*, 1908–1914.

(37) Briand, E.; Gu, C.; Boujday, S.; Salmain, M.; Herry, J. M.; Pradier, C. M. Functionalisation of gold surfaces with thiolate SAMs: Topography/bioactivity relationship − A combined FT-RAIRS, AFM and QCM investigation. *Surf. Sci.* **2007**, *601*, 3850–3855.

(38) Parra, A.; Casero, E.; Pariente, F.; Vazquez, L.; Lorenzo, E. Bioanalytical device based on cholesterol oxidase-bonded SAM-modified electrodes. *Anal. Bioanal. Chem.* **2007**, *388*, 1059–1067.

NOTE ADDED AFTER ASAP PUBLICATION

There were errors in Figure 2A, the caption of Figure 2, and the second paragraph of the Results and Discussion section of the version of this paper published May 18, 2011. The correct version published May 24, 2011.